

Vertical Transverse Coherence Properties of FLASH in Deep Saturation

Stefan Döge*

Supervisors[†]: Andrej Singer, Adrian Mancuso, Ivan Vartanians

*Universität Leipzig, Fakultät für Physik und Geowissenschaften, Linnéstraße 5, 04103 Leipzig

[†]HASYLAB at DESY, Notkestraße 85, 22607 Hamburg, Germany

September 10, 2010

This paper is the summary of the project assigned to me in the framework of the DESY Summer Student Program 2010. The project aimed at contributing to the data analysis of double slit diffraction patterns obtained from measurements at the free-electron laser called FLASH at the DESY research center in Hamburg, Germany. Eventually, the measurements carried out by Andrej Singer et al. and their analysis will reveal specific coherence properties of the FLASH X-ray source. These are of great interest for materials and biophysics research using radiation of that source.

PACS: 41.60.Cr, 42.25.Bs, 42.25.Kb

1 Motivation

Light waves need to be coherent in order to produce an interference pattern when they overlap. Interference is required in some imaging techniques, e.g. Coherent X-Ray Diffraction Imaging (CXDI). The greater the coherence length of a photon source, the larger objects can be investigated. One of the methods to measure coherence is the double slit experiment.

2 Theory (Young's Double Slit Experiment) [1], [2]

The description of diffraction relies on the interference of waves emanating from the same source taking different paths to the same point on a screen. In this description,

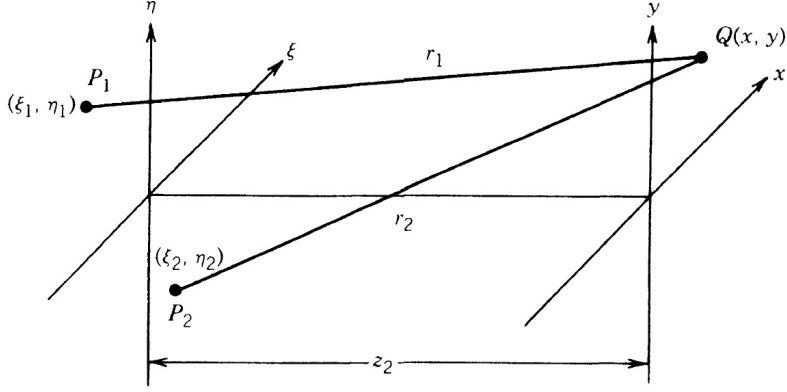


Figure 1: Interference geometry of the double slit experiment according to [1]

the difference in phase between waves that took different paths is only dependent on the effective path length. This does not take into account the fact that waves that arrive at the screen at the same time were emitted by the source at different times. The initial phase with which the source emits waves can change over time in an unpredictable way. This means that waves emitted by the source at times that are too far apart can no longer form a constant interference pattern, since the relation between their phases is no longer time-independent.

If waves are emitted from an extended source, this can lead to incoherence in the transverse direction. When looking at a cross section of a beam of light, the length over which the phase is correlated is called the transverse coherence length. In the case of Youngs double slit experiment, this means that if the transverse coherence length is smaller than the spacing between the two slits, the resulting pattern on the screen would look like two single slit diffraction patterns.

The wave source (end of last active FEL undulator) is located at a distance z_1 from the double slit, which is at a distance z_2 from the detector ($z_2 \ll z_1$). The optical axis is aligned with the axis Z, perpendicular to the XY plane as shown in Figure 1.

As the wave source is far away (z_1 is large), we assume that it is at infinity and the wavefront is incident parallel to the double slit. In those two slits (P_1 and P_2) it forms two analytical signals without delay. We want to know the intensity at point Q , located at a distance r_1 and r_2 with respect to P_1 and P_2

$$\mathbf{u}(Q, t) = \mathbf{K}_1 \mathbf{u} \left(P_1, t - \frac{r_1}{c} \right) + \mathbf{K}_2 \mathbf{u} \left(P_2, t - \frac{r_2}{c} \right), \quad (1)$$

where \mathbf{K}_1 and \mathbf{K}_2 are (possibly complex-valued) constants. We know that $I(Q) = \langle \mathbf{u}^*(Q, t) \mathbf{u}(Q, t) \rangle$ and with some algebra, we obtain the intensity

$$I(Q) = I^{(1)}(Q) + I^{(2)}(Q) + 2\mathbf{K}_1 \mathbf{K}_2 \text{Re} \left(\Gamma_{12} \left(\frac{r_1 - r_2}{c} \right) \right), \quad (2)$$

where $\Gamma_{12}(\tau) = \langle \mathbf{u}(P_1, t + \tau) \mathbf{u}^*(P_2, t) \rangle$ is the mutual coherence function of the light and plays a fundamental role in the theory of partial coherence.

Normalizing the coherence function using

$$\begin{aligned}\tilde{\gamma}_{12}(\tau) &= \frac{\Gamma_{12}(\tau)}{\{\Gamma_{11}(0)\Gamma_{22}(0)\}^{1/2}} \\ \tilde{\gamma}_{12} &= \gamma_{12}(\tau)e^{-i(2\pi\nu\tau - \alpha_{12}(\tau))}\end{aligned}\quad (3)$$

leads to

$$I(Q) = I^{(1)}(Q) + I^{(2)}(Q) + 2\sqrt{I^{(1)}(Q)I^{(2)}(Q)}\gamma_{12}\left(\frac{r_1 - r_2}{c}\right)\cos\left[2\pi\nu\frac{r_1 - r_2}{c} + \alpha_{12}\frac{r_1 - r_2}{c}\right]. \quad (4)$$

After substituting the following variables

$$\begin{aligned}r_1 &= \sqrt{z_2^2 + (\xi_1 - x)^2 + (\eta_1 - y)^2} \\ r_2 &= \sqrt{z_2^2 + (\xi_2 - x)^2 + (\eta_2 - y)^2} \\ \Delta\xi &= \xi_2 - \xi_1 \\ \Delta\eta &= \eta_2 - \eta_1 \\ d &= \sqrt{(\Delta\xi)^2 + (\Delta\eta)^2} \text{ (distance between slits),}\end{aligned}\quad (5)$$

where $\xi_{1,2}$ and $\eta_{1,2}$ are defined as in Figure 1 and assuming that the fringe contrast will be constant over the observation region of interest, we can simplify the mutual coherence function Γ_{12} and the complex degree of coherence γ_{12} . These functions can now be rewritten as

$$\begin{aligned}\Gamma_{12}(\tau) &\cong J_{12}e^{-i2\pi\tilde{\nu}\tau} \\ \gamma_{12}(\tau) &\cong \mu_{12}e^{-i2\pi\tilde{\nu}\tau},\end{aligned}\quad (6)$$

where $J_{12} \triangleq \Gamma_{12}(0)$ is the mutual intensity of light at pinholes P_1 and P_2 , and

$$\mu_{12} \triangleq \gamma_{12}(0) = \frac{J_{12}}{\sqrt{I(P_1)I(P_2)}} \quad (7)$$

is called the complex coherence factor of the light with the property $0 \leq |\mu_{12}| \leq 1$. Eventually, we obtain for the case of a double slit

$$I(x, y) = I^{(1)} + I^{(2)} + 2\sqrt{I^{(1)}I^{(2)}}|\mu_{12}|\cos\left[\frac{2\pi}{\lambda z_2}(\Delta\xi x + \Delta\eta y) + \phi_{12}\right], \quad (8)$$

where μ_{12} is as explained above, λ is the wavelength of the radiation and ϕ_{12} is the phase difference between the two light waves at their respective slit. $I^{(1)}$ and $I^{(2)}$ are the intensities of each slit as given by

$$I^{(1),(2)} = I_0^{(1),(2)}\text{sinc}\left[\frac{a}{\lambda z_2^2}x - \left(\frac{z_1 + z_2}{z_1}\right)\xi_{1,2}\right]^2, \quad (9)$$

where the normalized *sinc* function is defined as $\text{sinc } x = \frac{\sin(\pi x)}{\pi x}$, which we used, and sometimes as $\text{sinc } x = \frac{\sin(x)}{x}$. I_0 is the original beam intensity at the slit. In the following data analysis, the two slit intensities $I_0^{(1),(2)}$ were taken to be the same. It might be necessary for further refinement of the data fitting procedure to introduce another parameter that accounts for intensity differences at both slits. In that case one could write

$$\begin{aligned} I^{(1)} &= I_0^{(1),(2)} \text{sinc}(\dots), \\ I^{(2)} &= (1 + \text{para}(r)) I_0^{(1),(2)} \text{sinc}(\dots), \end{aligned} \tag{10}$$

where $I_0^{(1),(2)}$ is the intensity parameter used in the fitting program now and $\text{para}(r)$ represents the relative deviation of one intensity from the other.

So what is reported in this paper is the inference of the complex coherence factor $|\mu_{12}|$ from a given double slit separation and the measurement of the diffraction pattern produced by these slits.

3 Experimental Setup

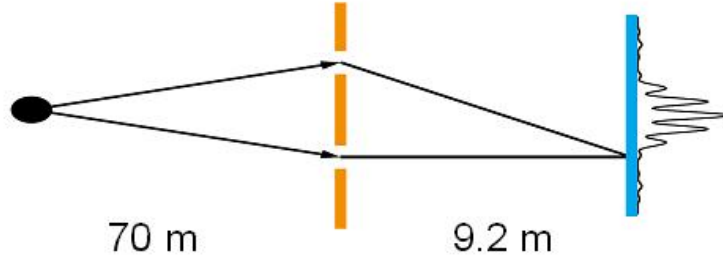


Figure 2: Setup of the Double Slit Experiment at FLASH, $z_1 = 70$ m, $z_2 = 9.2$ m

The double slit holder was at a distance of 70.0 meters downstream from the X-ray source, which is measured from the end of the last aligned (i.e. operating) undulator. Between the double slit and the pnCCD detector (courtesy of Max Planck Institute, Max-Planck-Arbeitsgruppen für strukturelle Molekularbiologie Hamburg) there was a 9.2 meter spacing. Originally, a spacing of 9.5 meters was recorded, but with the help of Equation 11 and the fact that the fitted slit distances were about 3.3 % too large, we corrected it down to 9.2 meters. The detector's pixel size was a squared $75 \mu\text{m}$ per pixel. Five undulator modules were operating and FLASH produced electron bunches of 50-55 μJ energy in deep saturation mode, which starts at about $40 \mu\text{J}$, and photons of 13.5 nm wavelength. The slits themselves were $10 \mu\text{m}$ wide and $50 \mu\text{m}$ high. Four different slit separations were used to create diffraction patterns: 150, 300, 350 and $500 \mu\text{m}$.

4 Finding Parameters

From the 2-dimensional diffraction pattern recorded by the CCD one can obtain a line plot (plots intensity vs. x range), which makes the intensity information accessible. This line plot can be drawn using the command `plot(a.imm(y1, x1:x2))`, where `a.imm` is the matrix containing the actual diffraction pattern, y_1 is the horizontal line through the diffraction pattern (counted from the top) and x_1 and x_2 select the horizontal range for the plot. In this example `plot(a.imm(105,:))` was selected, see Figures 3 and 4. From the spatial fringe period (distance between the top of two neighboring fringes – number of pixels times $75\mu\text{m}$) L_P (in μm) it is possible to calculate the distance d between the two pinholes according to

$$d = \frac{\lambda z_2}{L_P}, \quad (11)$$

where λ is the wavelength of the utilized radiation ($E = 91.9\text{eV} \hat{=} \lambda = 13.5\text{nm}$) and z_2 signifies the distance pinholes–screen (9.2m), according to Young’s double slit experiment [1]. The example measurement gives a spatial fringe period of $804.8\mu\text{m}$, which we count, and a pinhole–pinhole distance of $154.3\mu\text{m}$, which can be calculated using above formula. So, the farther the slits are separated the smaller the spatial fringe period. Other physical dimensions that are correlated to properties of the diffraction pattern are the shape of the envelope of the fringe pattern, which is connected to the slit width – the wider the slit the narrower the envelope –, the height of the envelope, which is directly proportional to the intensity at the slit (with $\gamma_{12} = \text{const.}$), and the ratio

$$\mathfrak{z} = \gamma_{12} = \frac{I_{\max} - I_{\min}}{I_{\max} + I_{\min}}, \quad (12)$$

which denotes the visibility of the fringes.

Double Slit Property	Diffraction Pattern
slit separation \uparrow	fringe period \downarrow
slit width \uparrow	(width) shape of envelope \downarrow
intensity $I_0 \uparrow$	height of envelope \uparrow
visibility $\gamma_{12} \uparrow$	$\mathfrak{z} = \frac{I_{\max} - I_{\min}}{I_{\max} + I_{\min}} \uparrow$

Table 1: Correlations between physical properties of the slits and diffraction pattern parameters

After the initial estimation of the fit parameters, the tilt of the fringe pattern, which arises from the slits not being exactly aligned horizontally, is determined by virtually extending a line through one of the fringes in the 2D pattern and noting the x-y-coordinates of two points along that line. In Figure 3 the two chosen points along the same fringe yield a Δx of -5 and a Δy of 119, which leads to a tilt angle of $\alpha = \arctan(-5/119) = -2.41^\circ$ respective the perpendicular (y-axis).

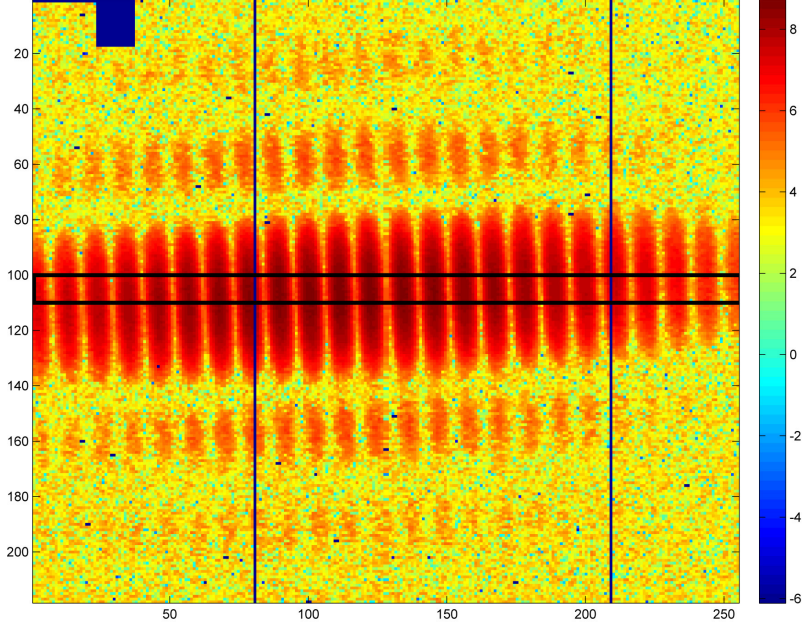


Figure 3: 2D diffraction pattern, slight tilt to the left, slit separation $150 \mu\text{m}$, fitting are in black rectangle, 20 fringes over a 215 pixels distance; the diffraction patterns above and below the main pattern are due to the finite slit height

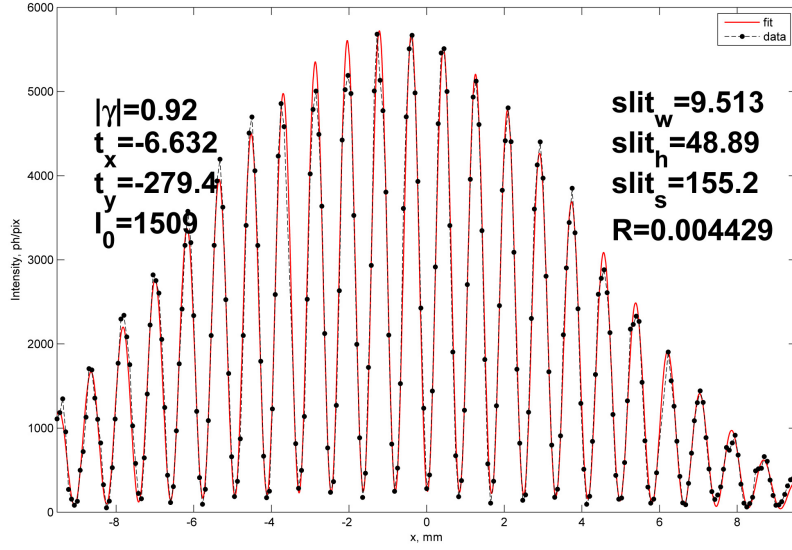


Figure 4: Fringe pattern (line plot) through center of marked fitting range in Figure 3

If a piecewise range is necessary for the fit – perhaps because of a beamstop or other interruption of the interference pattern –, then $\text{range_x} = [x_1:x_2, x_3:x_4]$ would be the

command to use. The fitting procedure outputs an error R defined as

$$R = \frac{\sum_{i=1}^N (I_i^{exp} - I_i^{fit})^2}{\sum_{i=1}^N (I_i^{fit})^2}, \quad (13)$$

which was smaller than 0.006 for each fit.

5 Data Fitting

The data fit (red) is shown in Figure 4. Initially, starting values for each parameter are estimated and minimum and maximum points are chosen. The fitting procedure then creates the best fit that obeys these constraints. The upper and lower boundaries need to be estimated as well and should be narrowed down as the fitting procedure is applied again and again. The parameters should be manipulated until none of them reaches its preset upper or lower boundary and the overall picture looks sound.

6 Results and Discussion

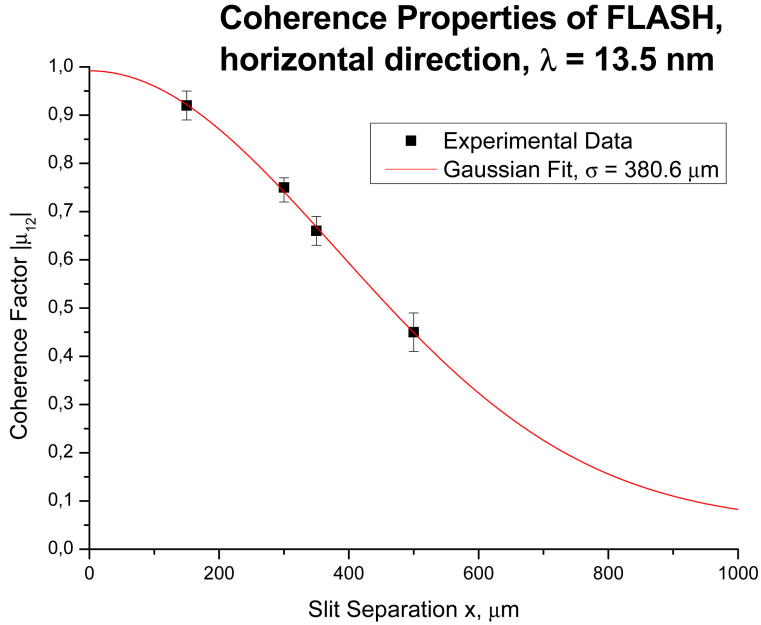


Figure 5: Root mean square (sigma) of the Gauss fit through the absolute value of the complex coherence factor $|\mu_{12}|(x)$ for slit separations of 150, 300, 350 and 500 μm ; corresponds to the coherence length of the X-ray source

The error bars in Figure 5 were calculated by fitting nine to ten 6-pixel tall 2D intervals from the top to the bottom of the main interference pattern as shown in Figure 3. This

was done for all for difference slit separations and the absolute deviation from the fit through the middle of the interference pattern was used as upper and lower error bounds.

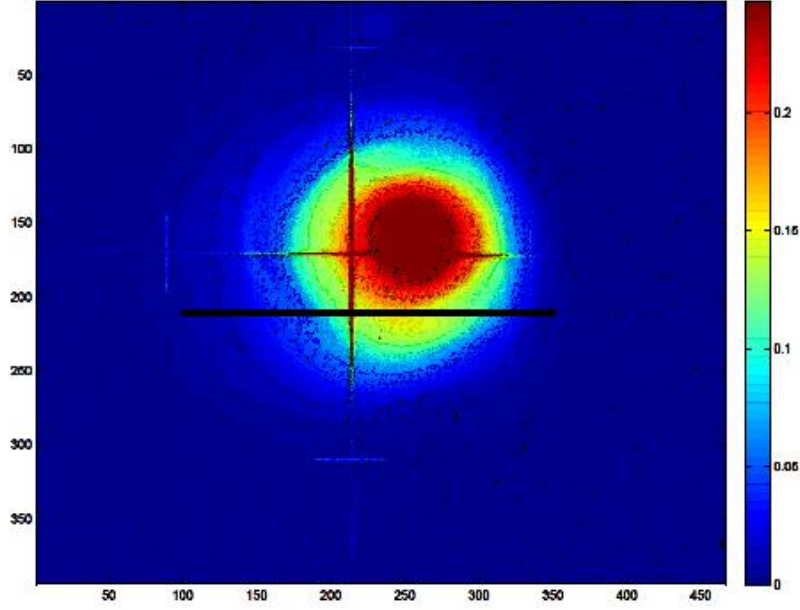


Figure 6: Direct beam 2D, as measured with a Ce-doped YAG scintillator crystal and a CCD camera

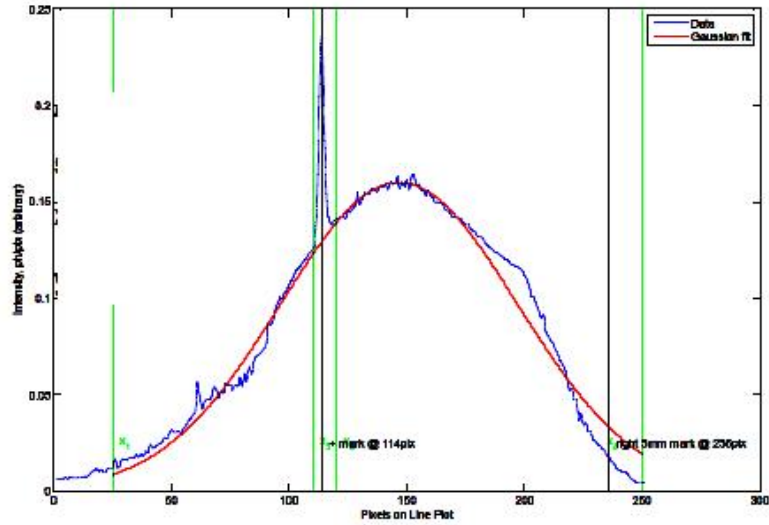


Figure 7: Line plot through the direct beam, Gaussian fit

In the end, the coherence factor $|\mu_{12}|$ alone tells little about the coherence properties of the X-ray source. It is possible to widen the beam and thereby increase its coherence length. That, however, is not desirable, since the a more divergent beam has less intensity

on the spot, so noise can infringe the measurement. It is thus highly desirable to know the coherence properties of a highly intense beam. The beam used for the discussed interference experiments was therefore radiated on a Ce-YAG scintillator crystal and captured with a CCD chip. Figure 6 shows the beam cross section, where red represents high intensity and blue low intensity. Several line plots (like in Figure 7) were taken from the 2D image and fitted with a Gaussian algorithm in order to estimate the beam's σ . It was found to be $\sigma = (1886 \pm 160) \mu m$.

From $\sigma_{coh} = \xi = 380 \mu m$ (root mean square of complex coherence factor $|\mu_{12}|(x)$) and $\sigma_{beam} = \sigma = (1900 \pm 200) \mu m$ (root mean square of the beam intensity) we can calculate the coherence quality factor

$$q = \frac{\xi}{\sigma} = 0.20 \pm 0.02 \quad (14)$$

and eventually the normalized degree of coherence

$$\zeta = \frac{q}{\sqrt{q^2 + 4}} = (10.0 \pm 1.5) \% \quad (15)$$

Andrej Singer et al.[3] published a normalized degree of coherence of 17% for the same X-ray source, but in their experiment the X-rays did not pass through any optical elements. So, from my analysis it can be concluded that the optical elements in the X-ray path may lead to some loss of coherence.

7 Additional Work to Be Done

During the data fitting the finite pixel size was not taken into consideration. That becomes especially obvious at the $500 \mu m$ slit separation sample. The line plot clearly shows data points shooting far out of the fitting range, which is not due to physics, but to the small number of measurement points per fringe. However, this shortcoming can be corrected mathematically/statistically.

References

- J. W. GOODMAN (2000). Statistical Optics. Wiley-Interscience, New York. p. 170ff.
- CARLOS PICÓ RUIZ (2009). [*Horizontal*] Transverse Coherence Properties at FLASH. Summer Student project report, DESY Hamburg.
- ANDREJ SINGER ET AL. (2008). Transverse-Coherence Properties of the Free-Electron-Laser FLASH at DESY, Phys. Rev. Lett. 101, 254801.

Appendix

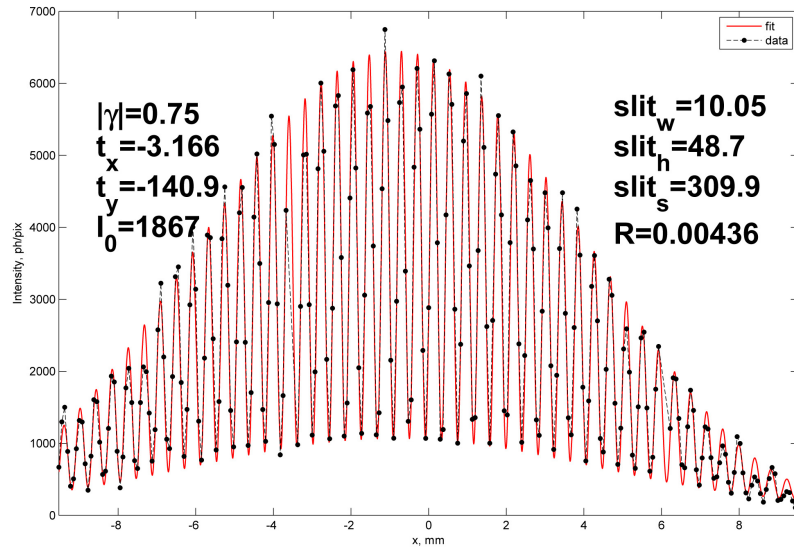


Figure 8: Line plot through center of 2D interference pattern, slit separation $300 \mu\text{m}$

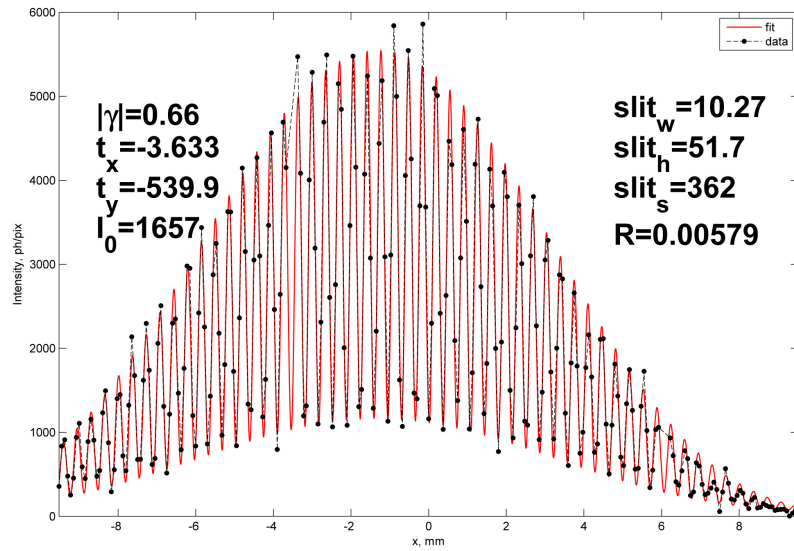


Figure 9: Line plot through center of 2D interference pattern, slit separation $350 \mu\text{m}$

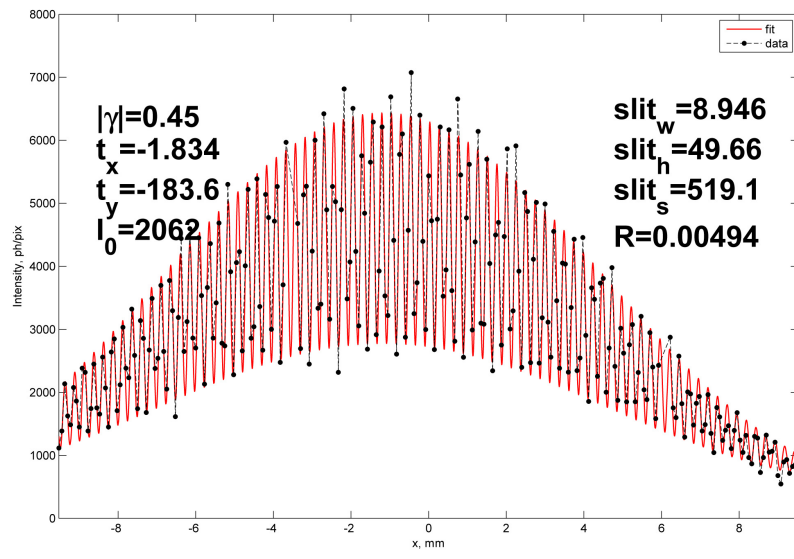


Figure 10: Line plot through center of 2D interference pattern, slit separation $500\ \mu\text{m}$